A new miniaturized wideband self-isolated two-port MIMO antenna for 5G millimeter-wave applications

Asma Khabba[1], Jamal Amadid[1], Layla Wakrim[2], Zakaria El Ouadi[1], Saida Ibnyaich[1], Ahmed Jamal Abdullah Al-Gburi[3], Abdelouhab Zeroual[1], Tole Sutikno[4]

[1]Instrumentation, Signals and Physical Systems (I2SP) Team, Department of Physics, Faculty of Sciences Semlalia, Cadi Ayyad University, Marrakesh, Morocco
[2]Laboratory of Innovation in Management and Engineering for Business (LIMIE), Higher Institute of Engineering and Business (ISGA), Marrakesh, Morocco
[3]Department of Electronic and Computer Engineering (FKEKK), Center of Telecommunication Research and Innovation (CeTRI), Universiti Teknikal Malaysia Melaka (UTeM), Durian Tunggal, Malacca, Malaysia
[4]Department of Electrical Engineering, Faculty of Industrial Technology, Universitas Ahmad Dahlan, Yogyakarta, Indonesia

Article Info

ABSTRACT

Nowadays, millimeter-wave frequencies present a catchy solution to securing the colossal data rate needed for 5G communications. Accordingly, this research deals with the conception of a novel orthogonal 2×2 multiple input, multiple output (MIMO) antenna design operating in the millimeter wave spectrum with quite small dimensions of $11 \times 6 \times 0.8$ mm^3. The single antenna element consists of a trapezoidal microstrip patch antenna built on the Rogers RT5880 laminate with a permittivity of 2.2 and tangent loss of 0.0009. A trapezoidal-slot ground plane is used to support the structure. The antenna resonates at 28 GHz with a large bandwidth of 4 GHz from 26 to 30 GHz, a good gain of up to 5 dB, and a high radiation efficiency of 99%. A strong isolation is achieved that surpasses 26 dB. Besides, a high diversity performance is achieved where the envelope correlation coefficient (ECC) is lower than 0.001, the diversity gain (DG) is greater than 10 dB, and the channel capacity loss (CCL) is no longer than 0.4 bit/s/Hz. The achieved outcomes prove the robustness of the suggested MIMO antenna and qualify it to be a strong candidate for 5G wireless devices.

Corresponding Author:

Asma Khabba
Instrumentation, Signals and Physical Systems (I2SP) Team, Department of Physics
Faculty of Sciences Semlalia, Cadi Ayyad University, Marrakesh, Morocco
Email: asma.khabba@edu.uca.ac.ma

1. INTRODUCTION

The rapid development and expansion of mobile terminals has resulted in an unprecedented increase in data traffic via internet technology. Hence, based on the Federal Communications Commission (FCC), the congestion in the microwave band may be eliminated by dedicating various bands in the millimeter-wave (mm-wave) spectrum beyond 24 GHz to execute the fifth-generation systems. Accordingly, many millimeter-wave frequency bands have been specified by the FCC, which include the pioneer bands, namely 27.5–28.35 GHz and 26.5–29.5 GHz around 28 GHz [1], [2]. The advantage of using the mm-wave band is its small size, which allows the incorporation of multiple antennas in a small space. However, the high-frequency spectrum is highly sensitive to weather conditions, which impacts the signals' transmission considerably owing to the severe path loss in the mm-wave bands compared to the microwave band, which can be addressed by implementing the concept of small cells together with using high-gain antennas [3]–[10].

In terms of its primary function of increasing data rate and channel capacity, the multiple-input multiple-output (MIMO) antenna is regarded as one of the most promising technologies for improving transmission quality at millimeter wave frequencies [11]–[17]. Therefore, plenty of research has been reported in the state of the art to suggest different MIMO antenna designs for the utilization of 5G wireless devices in the mm-wave spectrum. For instance, in [18], a two-element conventional patch MIMO antenna has been proposed for wearable applications at 24 GHz using an electromagnetic band gap (EBG) structure for gain improvement. However, the total size was 21.6×21.6 mm², which can be further miniaturized, and the bandwidth exhibited was only 0.8 GHz. Jilani *et al.* [19] presented a four-element coplanar waveguid (CPW) T-shaped MIMO antenna for ultra wide band (UWB) band applications. Nevertheless, the overall system occupied a sizeable area of 12×50.8 mm². In [20], a two-port modified patch MIMO antenna has been studied for dual-band operation. The antenna was providing a resonable bandwidth of 2.55 and 2.1 GHz at 28 and 38 GHz, respectively. But a low maximum gain of 1.83 dB was acheived. Similarly, in [21], a dual-band, two-port planar MIMO antenna has been suggested for the applications at 27 and 39 GHz. Although the antenna supported the wideband property, the total size was somewhat large, and only the ECC was treated to assess the MIMO performance. In [22], a substrate-integrated waveguide (SIW)-based 2-port MIMO antenna was investigated for 5G applications at the 28 GHz millimeter-wave spectrum. The MIMO design has provided a minimum isolation of 17 dB and a gain of up to 6.9 dB. Nonetheless, the bandwidth attained was only 0.4 GHz. In [23], a planar dual-element MIMO antenna has been suggested for employment at 28 GHz. The antenna was offering a reasonable gain of up to 7.88 dB. However, a relatively small bandwidth was exhibited, and a sizeable area has been occupied. Regarding the literature review above, various limitations have been observed in the reported designs, which are mainly represented by the large dimensions, small bandwidth, low gain, and complex structure that inherently reduce their suitability for the 5G systems. Accordingly, it is still needed to create a new MIMO antenna design that simultaneously combines the most coveted features, including small size, simple geometry, wide bandwidth, desirable radiation behavior, and high MIMO performance, which is the purpose of this study.

In this paper, a new 2×2 wideband MIMO antenna design with a common ground plane is suggested for 5G applications in the pioneering 28GHz band. The single antenna element is composed of a trapezoidal radiating element constructed on the low-loss Rogers RT/Duroid 5880 laminate ($\varepsilon_r = 2.2, tan\delta = 0.0009$) and backed by a slotted ground plane for miniaturization and bandwidth enhancement purposes. The intended design outperforms the other existing ones by virtue of its simple, compact, and tiny geometry, along with impressive performance, including a wide bandwidth and desirable radiation traits, besides assuring high MIMO competencies that make it a strong candidate for 5G systems. The rest of this paper is structured in the following manner: the single antenna design and performance are presented in section 2. The configuration and performance of the MIMO antenna are investigated in section 3. A comparison with the existing literature is performed in section 4. Finally, section 5 summarizes the study.

2. PROPOSED SINGLE ANTENNA DESIGN
2.1. Configuration of the antenna

The layout of the proposed antenna is manifested in Figure 1. As can be seen, the antenna is composed of a trapezoidal-shaped radiating plate alimented by a microstrip 50 Ω feeding line and built on the low-loss Rogers RT5880 laminate, characterized by a dielectric constant ε_r of 2.2, a low-loss tangent of 0.0009, and a thickness hs of 0.8 mm. The entire structure is then supported by a metallic ground plane with an etched trapezoidal slot. The overall antenna design is distinguished by its quite small dimensions of 5×6×0.8 mm³, while the final values of the remaining parameters are inserted in the same Figure 1. It is worth pointing out that the antenna structure was wisely and closely designed with fine-refinement of all the parameters to achieve the best results using the electromagnetic simulator well-known by computer simulation technology (CST) software.

2.2. Antenna evolution steps

Figure 2 presents the basic stepwise geometry that was followed to achieve the suggested design along with its corresponding frequency response. As shown in Figure 2(a), in the first stage, a conventional rectangular patch antenna (reference antenna) of width $Wp = 2.4$ mm and length $Lp = 2.2$ mm supported by a full uniform ground plane, has been carefully modeled using CST software based on the basic (1)-(4) [6]. As depicted in Figure 2(b), the second stage is executed by applying a triangular cut from both sides of the radiating patch which converts the conventional rectangular patch antenna to a trapezoidal antenna. Finally, as mentioned in Figure 2(c), the last step is accomplished by subtracting a trapezoidal-shaped slot from the ground plane beneath the radiating patch. While, the intended resonance is achieved after a careful adjustment of the slot dimensions. In order to comprehend the impact of each modification on the antenna response, Figure 2(d) presents the reflection coefficient of the antenna at each evolutionary step. As can be

seen, in the first stage, the initial antenna design has a resonant frequency at 34 GHz with a total bandwidth of 2.8 GHz, with reference to $|S11| \leq -10\ dB$, where the large bandwidth acquired is attributed to the small size of the radiating patch compared to the ground plane size. However, despite the broadband feature achieved, the reference antenna does not operate in the required 28 GHz band which necessitates further geometrical modification. Accordingly, the next steps are accomplished with the target to bring the resonant frequency at the desired frequency band with an improved bandwidth and optimized impedance matching. Hence, in the second stage, it can be seen that the executed cuts serve to shift the resonating frequency, i.e., 34 GHz, toward the lower frequency spectrum where it is settled at 33.2 GHz with an improved impedance matching and a full bandwidth of 2.2 GHz.

$$W_p = \frac{c}{2fr\sqrt{\frac{\varepsilon_r+1}{2}}} \tag{1}$$

$$\varepsilon_{eff} = \frac{\varepsilon_r+1}{2} + \frac{\varepsilon_r-1}{2}\left[1 + 12\left(\frac{h_s}{W_p}\right)\right]^{-1/2} \tag{2}$$

$$\Delta L = 0.421 h_s \frac{(\varepsilon_{eff}+0.3)\left(\frac{W_p}{h_s}+0.264\right)}{(\varepsilon_{eff}-0.258)\left(\frac{W_p}{h_s}+0.8\right)} \tag{3}$$

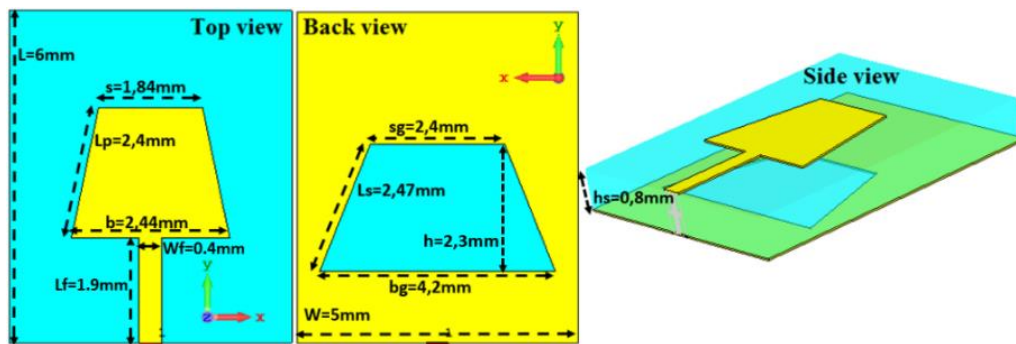$$L_p = \frac{c}{2fr\sqrt{\varepsilon_{eff}}} - 2\Delta L \tag{4}$$

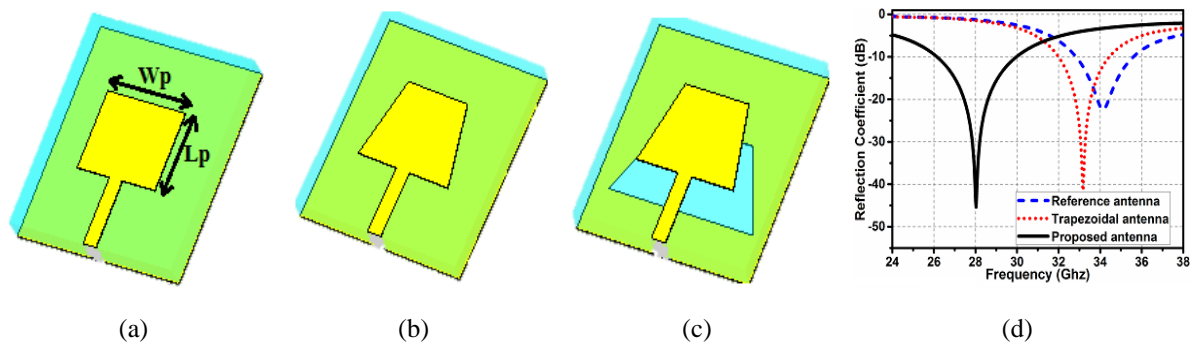Figure 1. Proposed antenna configuration

Figure 2. Evolution procedure of the proposed antenna: (a) reference antenna, (b) trapezoidal antenna, (c) proposed antenna, and (d) corresponding reflection coefficient

Thus, the ultimate step is executed with the intention to adjust the resonance at the desired frequency band. As illustrated, the trapezoidal slot has led to effectively altering the resonating frequency towards the lower frequency range until it was finally settled at the required frequency, i.e., 28 GHz with an improved bandwidth up to 4 GHz and high impedance matching where the reflection coefficient reaches a minimum value of -45 dB. Consequently, the proposed design succeeded in providing a wideband property in the 28 GHz band without needing to increase the overall dimensions.

To further investigate the antenna behavior, Figure 3 presents the electrical current distribution of the trapezoidal antenna with and without the trapezoidal slot. By observing the surface current distribution shown in Figure 3(a), it can be seen that the lateral cuts contribute to extend the electric current path along the radiating patch borders which increases the electrical length, conducting to decrease the resonating frequency. Furthermore, it can be observed that before etching the trapezoidal slot, the electric current is also concentrated in the ground directly beneath the patch owing to the coupling effect. The influence of the etched slot can be clearly remarked from the current distribution configured in Figure 3(b). As illustrated, after engraving the slot, it is observed that the current has trend to be intensified along the slot edges, as the later favour edges to go through. Therefore, the engraved slot serves to add extra edges for the current distribution, which further increased the antenna's electric length, leading to decrease the antenna resonant frequency.
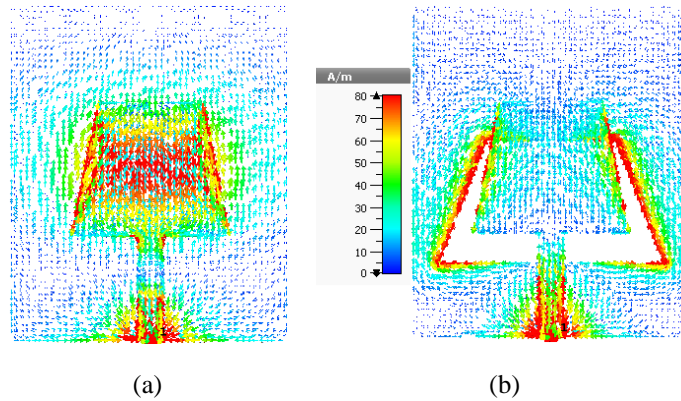

(a)   (b)

Figure 3. Current distribution of (a) trapezoidal antenna at 33.2 GHz and (b) proposed antenna at 28 GHz

2.3. Parametrical analysis of the trapezoidal slot

In order to well know the effect of the added slot on the antenna frequency response, Figure 4 illustrates the parametric study on the long base bg, short base sg and the height h of the slot. As appeared in Figure 4(a), when the long base bg is altered from 3.8 to 4.4 mm the resonant frequency is shifted from 28.5 GHz towards the lower frequency. Where the required resonance is detected when bg is 4.2 mm. The effect of the height h on the reflection coefficient is presented in Figure 4(b), as seen, when the height h is increased from 2.1 to 2.5 mm the resonant frequency is slightly affected. In contrast the impedance matching is remarkably changed while the best matching is attained when the height h is 2.3 mm. The influence of the short base sg is depicted in Figure 4(c), as manifested, the short base sg has a significant effect on the resonating frequency when it is swapped from 2 to 2.8 mm.
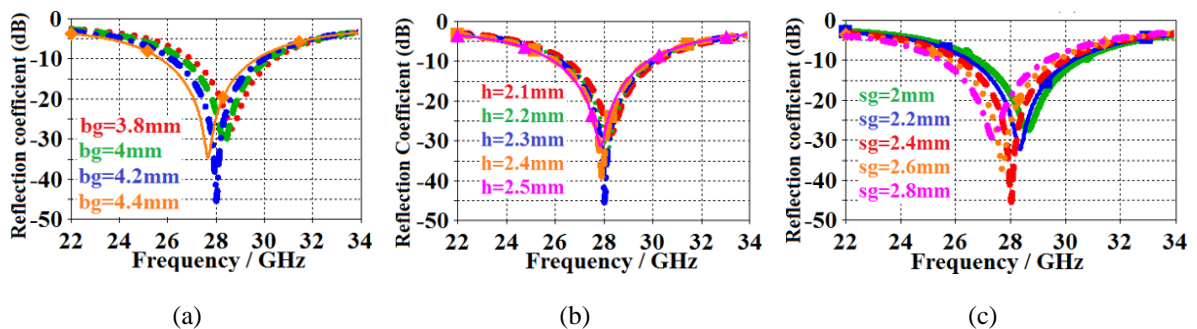

(a)   (b)   (c)

Figure 4. Parametrical study of various parameters related to the trapezoidal slot: (a) bg parameter, (b) h parameter, and (c) sg parameter

Where the resonance is decreased from 28.9 to 27.5 GHz and the optimized response is achieved when the short base sg is 2.4 mm. Consequently, the executed parametric analysis has proven the crucial role of the engraved slot parameters on the frequency response. Indeed, a careful tuning of the slot dimensions leads to the best possible antenna response.

2.4. Results and discussions

Figure 5(a) plots the reflection coefficient (S11) of the suggested design, which is generated using two computational tools, namely CST and high frequency structure simulator (HFSS) software, for validation purpose. As reported, the extracted curves demonstrate a great compatibility with an insignificant discrepancy, which can be due to the different computational methods adopted by both simulators. A pretty-good operation is shown, where the antenna resonates at the prominent frequency band of 28 GHz and has a large band characteristic of 4 GHz from 26 GHz to 30 GHz, which includes some of the most promising bands for the 5G systems such as 27.5–28.35 GHz, 26.5–29.5 GHz, and 27.5–29.5 GHz. Hence, the suggested antenna is capable of operating in different geographical areas.

The input impedance of the suggested antenna is depicted in Figure 5(b). The antenna input impedance is defined by a complex number, where the real part is the antenna resistance and the imaginary part is the reactance of the antenna. Therefore, for a good impedance match at a certain frequency, the resistance should be around 50 Ω while the reactance must be close to 0 Ω. As revealed in Figure 5(b), at the resonance frequency, i.e., 28 GHz, the resistance is 49.4 Ω and the reactance is -0.34 Ω, which assures a good matching property. Figure 6 depicts the radiation performance of the proposed antenna. Figure 6(a) displays the two-dimensional radiation pattern in the E-plane (YOZ) and H-plane (XOZ) at different frequencies, namely 26 GHz, 28 GHz, and 29 GHz.
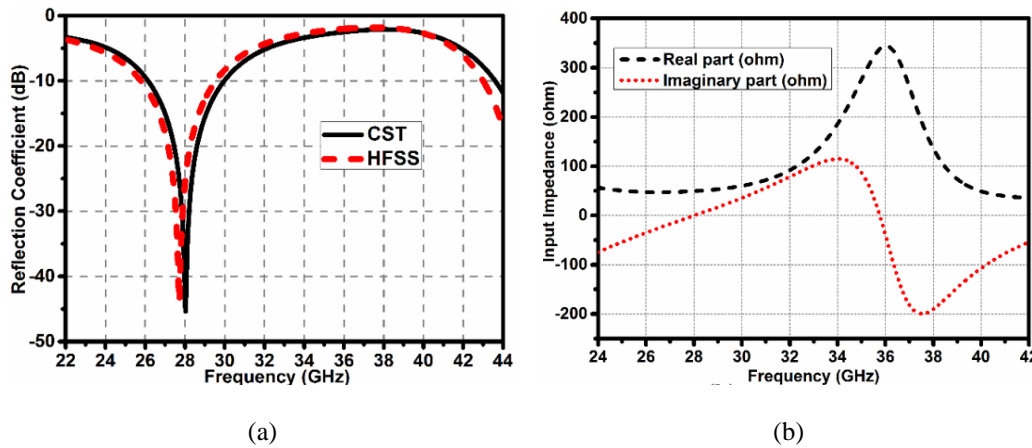

(a)   (b)

Figure 5. Impedance characteristics: (a) reflection coefficient of the suggested antenna and (b) input impedance

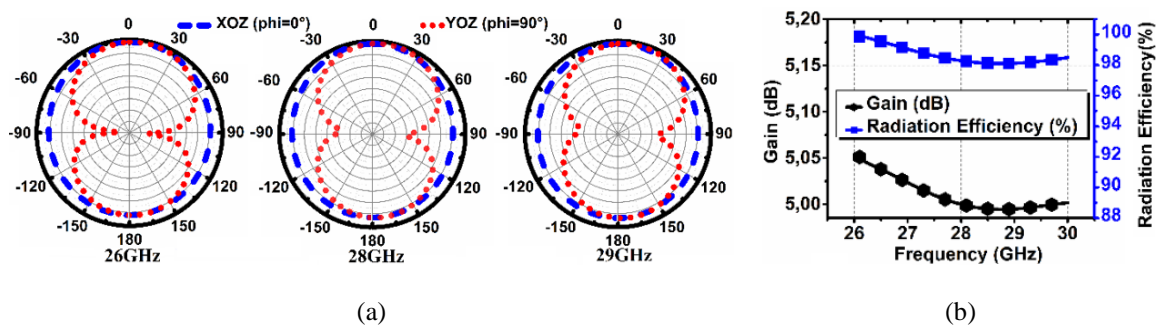(a)   (b)

Figure 6. The proposed antenna: (a) 2D radiation pattern at various frequencies and (b) gain and radiation efficiency vs frequency

As revealed, at the three selected frequencies, the suggested antenna shows good radiation behavior in both cutting planes. Indeed, it is noted that the antenna preserves a bidirectional and omnidirectional pattern in the E and H planes, respectively, which proves a stable and uniform radiation performance. Figure 6(b) depicts the gain and radiation efficiency over frequency. A good radiation characteristics are observed across the entire operating band where the gain is set at 5 dB and the radiation efficiency ranges from between 98 and 99%.

3. MIMO ANTENNA DESIGN

3.1. Proposed configuration and S-parameters

Given the necessity of the MIMO antenna to realize 5G technology and its significant role in ensuring high data rate throughput, this section is assigned to propose a MIMO system based on the single antenna discussed above. As shown in Figure 7, the MIMO antenna is made up of two units of a single antenna that are placed orthogonally on the same Rogers 5880 and have a total size of 11×6 mm^2. The orthogonal placement serves to provide polarization diversity, which in turn helps to enhance the isolation. Furthermore, the proposed configuration supports the common ground plane structure, which is required for its practical use and integration with other components in wireless devices. As reported in the same figure, the MIMO assembly does not affect the individual performance of elements. Indeed, both elements exhibit very good performance in terms of reflection coefficient and mutual coupling, where a large operating band from 26 GHz to 30 GHz is borne with a weak mutual coupling lower than -26 dB in the whole band, which certainly contributes to highly isolated MIMO elements.
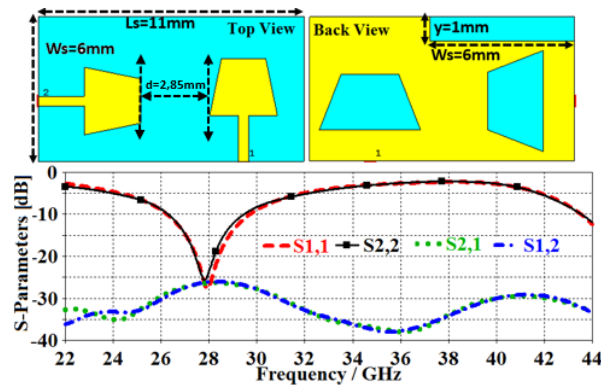
Figure 7. Layout of the MIMO antenna along with its resulting S-parameters

3.2. Effect of the orthogonal placement

In order to recognize the effect of the orthogonal arrangement, Figure 8 shows two different MIMO structures, namely, parallel and orthogonal (proposed) structures, together with their corresponding mutual coupling. The radiating plates are separated by the same distance for both structures. As seen, the orthogonal structure shows a high isolation level exceeding 26 dB as compared with the traditional parallel placement, where a low minimum isolation of only 17.5 dB is reached in the band of interest of 26–30 GHz. As a result, the use of orthogonal arrangements resulted in a significantly improved minimum isolation of 8.5 dB without the need for any design modifications. This isolation improvement in the orthogonal MIMO antenna is due to the polarization diversity where the E-field vectors have a perpendicular orientation, which inherently minimizes the coupling energy among elements and increases their isolation.
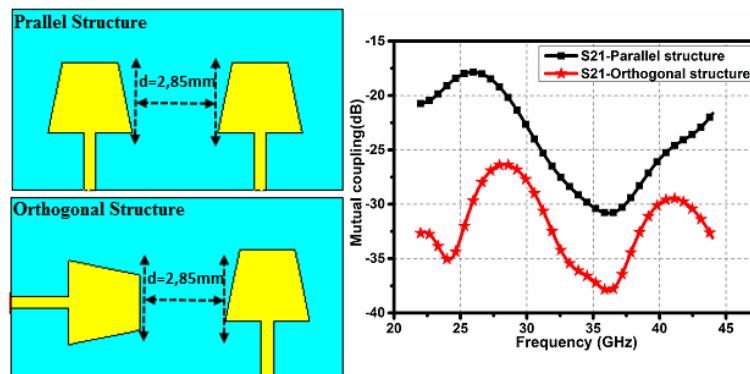

Figure 8. Mutual coupling of different MIMO structures

3.3. Radiation pattern

Figure 9 displays the two-dimensional radiation pattern in the E (YZ) and H (XZ) planes for the two MIMO elements at 26 GHz, 28 GHz, and 30 GHz. As can be seen, the MIMO antenna preserves good radiation behavior in both cutting planes, which is not strongly affected by MIMO composition. Furthermore, it can be noted that the radiation pattern of one antenna element is reversed for the other element. In other words, the E-plane and H-plane of Ant1 are in reverse order for Ant2, which is referred to as the phenomenon of polarization diversity and which can help to provide uncorrelated patterns for a good communication system.
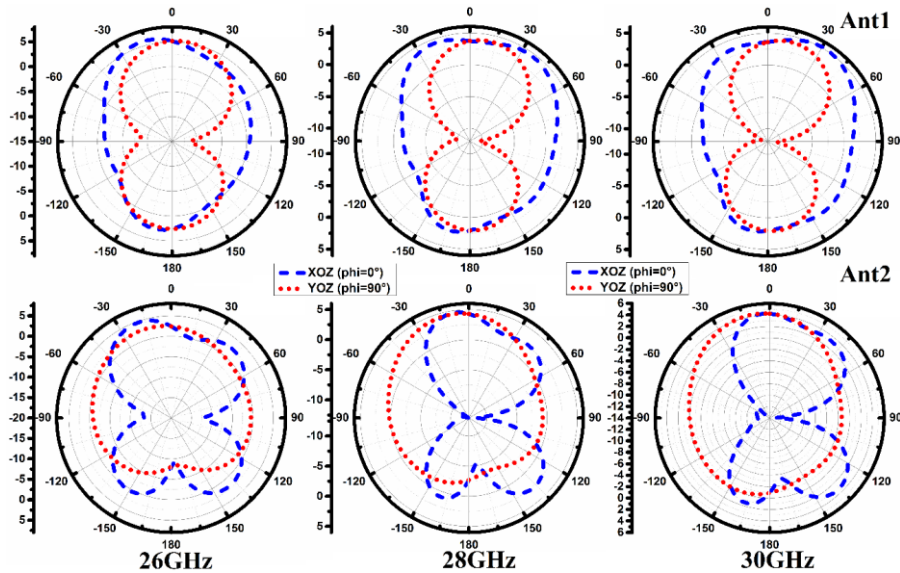
Figure 9. 2D-radiation pattern for both MIMO elements at three selected frequencies

3.4. Diversity performance

In order to well study the proposed MIMO system, the diversity performance of MIMO antenna has been studied in term of the envelope correlation coefficient (ECC), diversity gain (DG), and channel capacity loss (CCL) which are presented in Figure 10. The ECC measures the correlation between the MIMO elements which should be less than 0.5 for a good MIMO performance and highly uncorrelated system. It can be calculated by the S-parameters using (5) [8].

$$ECC = \frac{|S_{11}^* S_{12} + S_{21}^* S_{22}|^2}{(1-(|S_{11}|^2+|S_{21}|^2))(1-(|S_{22}|^2+|S_{12}|^2))} \tag{5}$$

As remarked in Figure 10(a), the ECC of the MIMO antenna is below 0.001 which largely fulfill the industrial requirement. Another crucial metric to be assessed is the diversity gain, which defines the amelioration of signal to noise ratio when a diversity scheme is applied [2]. It can be determined using the ECC as formulated by (6) [11]. According to (6), the lower is the ECC the higher is DG. For high MIMO performance, the DG should be near to 10 dB, as seen in Figure 10(a), the DG is higher than 9.99 dB across the operational band and reaches a maximum value of 10 dB at the resonant frequency which proves high MIMO diversity performance. One other crutial metric to be assessed is the CCL. This parameter describes the maximum permissible loss in bit/s/Hz, at which the signals can be reliably transmitted [24], [25]. It can be computed using (7). In the practical case, the CCL should be less than 0.4 bit/s/Hz to assure a high transmitting rate.

$$DG = 10\sqrt{1 - ECC} \tag{6}$$

$$C_{loss} = -\log_2 \det(\alpha^R) \tag{7}$$

Where $\alpha^R = \begin{bmatrix} \alpha_{11} & \alpha_{12} \\ \alpha_{21} & \alpha_{22} \end{bmatrix}$, $\alpha_{ii} = 1 - \left(|S_{ii}|^2 + |S_{ij}|^2 \right)$ and $\alpha_{ij} = -\left(S_{ii}^* S_{ij} + S_{ji}^* S_{ij} \right)$ with $i, j = 1$ or 2.

The calculated CCL is reported in Figure 10(b). As can be seen, the proposed structure shows a very good performance, where the corresponding CCL is well below 0.4 bit/s/Hz over the operating bandwidth and reaches a minimum value close to 0 at the resonating frequency. Hence, the achieved outcome proves the ability of the intended design to fulfill a reliable communication.
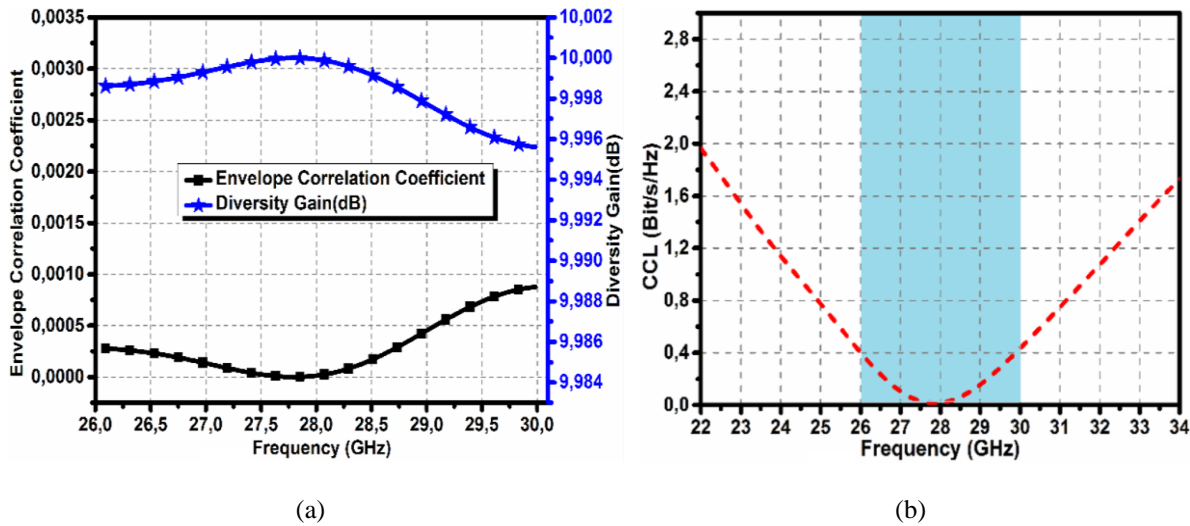

(a)   (b)

Figure 10. Diversity performance of the MIMO antenna along the operating band: (a) ECC and DG and (b) CCL

4. COMPARISON WITH SOME RELEVANT RESEARCH

In this section, the suggested design is thoughtfully compared with other related state-of-the-art designs in terms of various standards, and the comparative study is summarized in Table 1. There is no doubt that the published research contains an infinite number of reports that present various MIMO antenna designs for millimeter-wave 5G systems. However, if one looks at the table of comparison that is provided below, they will see that the design that has been proposed is superior to the designs that have been mentioned in a number of significant ways. In point of fact, the MIMO design that we have proposed has the smallest size and the highest radiation efficiency in addition to bearing a broad bandwidth and high isolation. Additionally, it can be seen that the proposed design maintains a good comparable gain and diversity performance that is satisfactory, whereas the majority of configurations are not examined in terms of CCL. In addition, the usability of some of the works that were reported, such as [20], [21], [26] [27], was hindered because they did not use the common ground structure. Because of this, the accomplishments demonstrate that the proposed structure has a high potential to become a suitable candidate for 5G application because it provides attractive performance in comparison to other designs that are of a larger size.

Table 1. Comparison with other existing literature

Ref.	Size (mm³)	Number of elements	Bandwidth (GHz)	Frequency range (GHz)	Gain (dB)/ efficiency (%)	Isolation (dB)	ECC/DG (dB)	CCL (bit/s/ Hz)
[12]	35×11×1.6	3	14	26–40	>5 / >70	>20	<0.01 / >9.9	NA
[18]	19.04×15.06×0.254	2	0.8	24 GHz-band	>4 / >70	>30	<0.24 / >9.6	NA
[20]	14×26×0.38	2	2.55	26.65–29.2	>0.5 / >76	>20	<0.01 / >9.99	<0.4
[21]	26×11 mm²	2	4	25–29	>3.5 / >97	>20	<0.001/ >9.99	NA
[22]	33×27.5×0.76	1 (2 ports)	0.4	28 GHz-band	6.9 / 87 (at 28 GHz)	>17	<0.2 / >9.7	NA
[23]	55×110×0.5	2	1.06	27.6–28.66	7.8 / 89 (at 28 GHz)	>29	<0.001/ NA	NA
[24]	11×21.7×0.254	2	2.29	25.5–27.79	5 / >90	>30	<0.122 / >9.91	<0.5
[26]	27.65×12×0.203	2	1.9	27.5–29.4	>5 / NA	>20	<0.002 / >9.99	NA
[27]	20×20×0.254	2	0.6	27.9–28.5	4.5 / NA	>30	<0.055 / >9.91	NA
[28]	120×60×0.5	2	0.5	27.8–28.3	8.2 / >85	>25	<0.014 / >9.99	NA
This work	11×6×0.8	2	4	26–30	>5 / >98	>26	<0.001 / >9.99	<0.4

5.   CONCLUSION

The purpose of this paper was to investigate the feasibility of constructing a MIMO antenna that is compact, uncomplicated, and of a quite-small size. The MIMO antenna performed exceptionally well, exhibiting desirable radiation characteristics as well as a broad operating band at 28 GHz. A high level of isolation is maintained by the MIMO elements, which is another factor that contributes to the system's high diversity performance. The overall results were compared to other works that were already published, which confirmed that the proposed MIMO antenna design is suitable for use in 5G millimeter wave applications.

REFERENCES

[1]   J. Khan, S. Ullah, U. Ali, F. A. Tahir, I. Peter, and L. Matekovits, "Design of a millimeter-wave mimo antenna array for 5G communication terminals," *Sensors*, vol. 22, no. 7, 2022, doi: 10.3390/s22072768.

[2]   A. Khabba, L. Wakrim, S. Ibnyaich, and M. M. Hassani, "Beam-Steerable Ultra-Wide-Band Miniaturized Elliptical Phased Array Antenna Using Inverted-L-Shaped Modified Inset Feed and Defected Ground Structure for 5G Smartphones Millimeter-Wave Applications," *Wireless Personal Communications*, vol. 125, pp. 3801–3833, 2022, doi: 10.1007/s11277-022-09737-4.

[3]   B. Aghoutane, S. Das, M. E. L. Ghzaoui, B. T. P. Madhav, and H. El Faylali, "A novel dual band high gain 4-port millimeter wave MIMO antenna array for 28/37 GHz 5G applications," *AEU - International Journal of Electronics and Communications*, vol. 145, 2022, doi: 10.1016/j.aeue.2021.154071.

[4]   S. -E. Didi, I. Halkhams, M. Fattah, Y. Balboul, S. Mazer, and M. El Bekkali, "Design of a microstrip antenna patch with a rectangular slot for 5G applications operating at 28 GHz," *TELKOMNIKA (Telecommunication, Computing, Electronics and Control)*, vol. 20, no. 3, pp. 527–536, 2022, doi: 10.12928/telkomnika.v20i3.23159.

[5]   O. A. Shareef, A. M. A. Sabaawi, K. S. Muttair, M. F. Mosleh, and M. B. Almashhdany, "Design of multi-band millimeter wave antenna for 5G smartphones," *Indonesian Journal of Electrical Engineering and Computer Science (IJEECS)*, vol. 25, no. 1, pp. 382–387, 2022, doi: 10.11591/ijeecs.v25.i1.pp382-387.

[6]   A. Khabba, S. Mohapatra, L. Wakrim, F. Ez-zaki, S. Ibnyaich, and A. Zeroual, "Multiband antenna design with high gain and robust spherical coverage using a new 3D phased array structure for 5G mobile phone MM-wave applications," *Analog Integrated Circuits and Signal Processing.*, vol. 110, pp. 331–348, 2022, doi: 10.1007/s10470-021-01954-4.

[7]   A. Khabba, S. Errahili, S. Ibnyaich, and M. M. Hassani, "A Novel Design of Miniaturized Leaf Shaped Antenna For 5G Mobile phones," in *Proceedings of the 3rd International Conference on Networking, Information Systems & Security*, 2020, no. 59, pp. 1–5, doi: 10.1145/3386723.3387878.

[8]   J. Kim and H. L. Lee, "High Gain Planar Segmented Antenna for mmWave Phased Array Applications," in *IEEE Transactions on Antennas and Propagation*, vol. 70, no. 7, pp. 5918-5922, 2022, doi: 10.1109/TAP.2022.3142333.

[9]   A. Gaya, M. H. Jamaluddin, and A. A. Althuwayb, "Wideband Millimeter wave Rectangular Dielectric Resonator Antenna with annular feed structure for 5G Applications," 2020 *IEEE International RF and Microwave Conference (RFM)*, 2020, pp. 1-4, doi: 10.1109/RFM50841.2020.9344771.

[10]   M. M. S. Altufaili, A. N. Najaf, and Z. S. Idan, "Design of circular-shaped microstrip patch antenna for 5G applications," *TELKOMNIKA (Telecommunication, Computing, Electronics and Control)*, vol. 20, no. 1, pp. 19–26, 2022, doi: 10.12928/telkomnika.v20i1.21019.

[11]   A. Khabba, S. Errahili, S. Ibnyaich, and A. Zeroual, "A New 2x2MIMO Trapezoidal Shaped Antenna with High Gain and Wide Bandwidth for 37-40GHz Millimeter Wave Applications," in *Proceedings of the 4th International Conference on Networking, Information Systems & Security*, 2021, no. 12, pp. 1–7, doi: 10.1145/3454127.3456584.

[12]   A. Patel *et al.*, "Inverted-L Shaped Wideband MIMO Antenna for Millimeter-Wave 5G Applications," *Electronics*, vol. 11, no. 9, 2022, doi: 10.3390/electronics11091387.

[13]   H. Askari, N. Hussain, M. A. Sufian, S. M. Lee, and N. Kim, "A Wideband Circularly Polarized Magnetoelectric Dipole Antenna for 5G Millimeter-Wave Communications," *Sensors*, vol. 22, no. 6, 2022, doi: 10.3390/s22062338.

[14]   A. Khabba, J. Amadid, S. Ibnyaich, and A. Zeroual, "Pretty-small four-port dual-wideband 28/38 GHz MIMO antenna with robust isolation and high diversity performance for millimeter-wave 5G wireless systems," *Analog Integrated Circuits and Signal Processing*, vol. 112, pp. 83–102, 2022, doi: 10.1007/s10470-022-02045-8.

[15]   A. Ahmad, D. -Y. Choi, and S. Ullah, "A compact two elements MIMO antenna for 5G communication," *Scientific Reports*, vol. 12, 2022, doi: 10.1038/s41598-022-07579-5.

[16]   P. Sagar and B. Jaymin, "Near optimal receive antenna selection scheme for MIMO system under spatially correlated channel," *International Journal of Electrical and Computer Engineering (IJECE)*, vol. 8, no. 5, pp. 3732–3739, 2018, doi: 10.11591/ijece.v8i5.pp3732-3739.

[17]   S. Patel *et al.*, "Impact of antenna spacing on Differential Spatial Modulation and Spatial Modulation for 5G-Based Compact Wireless Devices," *2021 4th International Symposium on Advanced Electrical and Communication Technologies (ISAECT)*, 2021, pp. 01-06, doi: 10.1109/ISAECT53699.2021.9668400.

[18]   A. Iqbal *et al.*, "Electromagnetic Bandgap Backed Millimeter-Wave MIMO Antenna for Wearable Applications," in *IEEE Access*, vol. 7, pp. 111135-111144, 2019, doi: 10.1109/ACCESS.2019.2933913.

[19]   S. F. Jilani and A. Alomainy, "Millimetre-wave T-shaped MIMO antenna with defected ground structures for 5G cellular networks," *IET Microwaves, Antennas & Propagation*, vol. 12, no. 5, pp. 672–677, 2018, doi: 10.1049/iet-map.2017.0467.

[20]   M. N. Hasan, S. Bashir, and S. Chu, "Dual band omnidirectional millimeter wave antenna for 5G communications," *Journal of Electromagnetic Waves and Applications*, vol. 33, no. 12, pp. 1581–1590, 2019, doi: 10.1080/09205071.2019.1617790.

[21]   W. Ali, S. Das, H. Medkour, and S. Lakrit, "Planar dual-band 27/39 GHz millimeter-wave MIMO antenna for 5G applications," *Microsystem Technologies*, vol. 27, no. 1, pp. 283–292, 2021, doi: 10.1007/s00542-020-04951-1.

[22]   M. Usman, E. Kobal, J. Nasir, Y. Zhu, C. Yu and A. Zhu, "Compact SIW Fed Dual-Port Single Element Annular Slot MIMO Antenna for 5G mmWave Applications," in *IEEE Access*, vol. 9, pp. 91995-92002, 2021, doi: 10.1109/ACCESS.2021.3091835.

[23]   H. M. Marzouk, M. I. Ahmed, and A. H. A. Shaalan, "Novel dual-band 28/38 GHz MIMO antennas for 5G mobile applications," *Progress In Electromagnetics Research C*, vol. 93, pp. 103–117, 2019, doi: 10.2528/PIERC19032303.

[24]   A. Kumar, A. K. Dwivedi, K. N. Nagesh, A. Sharma, and P. Ranjan, "Circularly Polarised Dielectric Resonator based Two Port Filtenna for Millimeter-Wave 5G Communication System," *IETE Technical Review*, vol. 39, no. 6, pp. 1501-1511, 2022, doi: 10.1080/02564602.2022.2028588.

[25] M. Bilal, S. I. Naqvi, N. Hussain, Y. Amin, and N. Kim, "High-Isolation MIMO antenna for 5G millimeter-wave communication systems," *Electronics*, vol. 11, no. 6, 2022, doi: 10.3390/electronics11060962.

[26] A. R. Sabek, W. A. E. Ali, and A. A. Ibrahim, "Minimally Coupled Two-Element MIMO Antenna with Dual Band (28/38 GHz) for 5G Wireless Communications," *Journal of Infrared, Millimeter, and Terahertz Waves*, vol. 43, pp. 335–348, 2022, doi: 10.1007/s10762-022-00857-3.

[27] D. Sharma, R. Katiyar, A. K. Dwivedi, K. N. Nagesh, A. Sharma, and P. Ranjan, "Dielectric resonator-based two-port filtennas with pattern and space diversity for 5G IoT applications," *International Journal of Microwave and Wireless Technologies*, pp. 1–8, 2022, doi: 10.1017/S1759078722000150.

[28] R. Hussain *et al.*, "A Multiband Shared Aperture MIMO Antenna for Millimeter-Wave and Sub-6GHz 5G Applications," *Sensors*, vol. 22, no. 5, 2022, doi: 10.3390/s22051808.

BIOGRAPHIES OF AUTHORS

Asma Khabba received the B.S. in physics and the Master degree in control, industrial computing, signals and systems in 2015 and 2017 respectively from Cadi Ayyad University. She is currently pursuing her studies to accomplish the Ph.D. degree in telecommunication and signal processing at Cady Ayyad University, Marrakech, Morocco. Her research interests include` 5G antenna, microwave/millimeter wave antenna, phased array and MIMO antenna. She can be contacted at email: asma.khabba@edu.uca.ac.ma.

Jamal Amadid got the B.S. in physics and the MS degree in control, industrial computing, signals and systems from Cadi Ayyad University in 2016 and 2019 respectively. Currently, he is continuing his study to complete the Ph.D. degree. His main research interests are: Massive-MIMO network, Channel Estimation for spatial correlated channels, pilot contamination and the cell-free Massive-MIMO in the 5G wireless communications system. He can be contacted at email: jamal.amadid@edu.uca.ac.ma.

Layla Wakrim received the B.S. in electrical engineering and the MS in electronics in 2010 from Cadi Ayyad University Marrakesh, Morocco. In 2018, she got the Ph.D. degree in telecommunication and signal processing at the same university. She is currently a full professor at the Higher Institute of Management and Business (ISGA), Marrakech Morocco. Her main research interests includes the antenna designs using genetic algorithm, telecommunication and signal processing. She can be contacted at email: layla.wakrim@isga.ma.

Zakaria El Ouadi received a B.S. degree in electronics in 2018 from the Cadi Ayyad University, Marrakech, Morocco. In 2020, he received the M.S. degree in Control, Industrial Computer, Signals, and Physical Systems from Cadi Ayyad University of Marrakesh, Morocco. He is currently a Ph.D. student in Telecommunications Engineering at the Cadi Ayyad University of Marrakesh, Morocco. His main research interest includes the filter nozzle design for 5G applications. He can be contacted at email: zakaria.elouadi@edu.uca.ac.ma.

Saida Ibnyaich 🆔 §ᴳ ꜱᴄ ꞇ is currently a professor at Cadi Ayyad University, Marrakesh, Morocco. She received the Bachelor degree in technical sciences, the Master degree in Electrical Engineering, Power Electronics, and Industrial Control, and the PhD degree in computing and telecommunication in 2002, 2005, and 2013, respectively, from Cadi Ayyad University. Her research interests include telecommunications, microwaves, millimeter waves, PIFA antennas, and patch antennas. She can be contacted at email: s.ibnyaich@uca.ac.ma.

Ahmed Jamal Abdullah Al-Gburi 🆔 §ᴳ ꜱᴄ ꞇ received M.Eng. and PhD degrees in Electronics and Computer Engineering (Telecommunication Systems) from Universiti Teknikal Malaysia Melaka (UTeM), Malaysia, in 2017 and 2021, respectively. He is currently a postdoctoral fellow with the Microwave Research Group (MRG), Faculty of Electronics and Computer Engineering, UTeM University. He has authored and co-authored a number of WoS and Scopus journals. His research interests include antennas, microwave sensors, and machine learning. He can be contacted at email: ahmedjamal@utem.edu.my.

Abdelouhab Zeroual 🆔 §ᴳ ꜱᴄ ꞇ is a professor of telecommunication systems and signal processing. He is the head of the Instrumentation, Signals, and Systems Team at the Faculty of Sciences Semlalia, Cadi Ayyad University in Marrakesh, Morocco. He received his Ph.D. degree in 1995 from Cadi Ayyad University. He supervises several research projects and serves as a reviewer for a number of international journals. His research interests include instrumentation, solar energy, signal processing, and wireless communications. He has published more than 140 conference papers and more than 60 journal papers. He can be contacted at email: zeroual@edu.uca.ac.ma.

Tole Sutikno 🆔 §ᴳ ꜱᴄ ꞇ is currently employed as a lecturer in the Electrical Engineering Department at Universitas Ahmad Dahlan (UAD), which is located in Yogyakarta, Indonesia. In 1999, 2004, and 2016, he graduated with a Bachelor of Engineering from Universitas Diponegoro, a Master of Engineering from Universitas Gadjah Mada, and a Doctor of Philosophy in Electrical Engineering from Universiti Teknologi Malaysia. All three degrees are in the field of electrical engineering. Since the year 2008, he has held the position of Associate Professor at the University of Ahmad Dahlan in Yogyakarta, Indonesia. His research interests include the areas of digital design, industrial applications, industrial electronics, industrial informatics, power electronics, motor drives, renewable energy, FPGA applications, embedded systems, artificial intelligence, intelligent control, digital libraries, and information technology. He can be contacted at email: tole@te.uad.ac.id.